



Fermi National Accelerator Laboratory

FERMILAB-Conf-81/28-THY
March 1981

ζ -Spectroscopy Beyond 40 GeV*

W. BUCHMÜLLER
Fermi National Accelerator Laboratory
P.O. Box 500, Batavia, Illinois 60510

*Presented at the "Z⁰ Physics" Workshop, Cornell University, Ithaca, New York,
February 6-8, 1981.



ζ -Spectroscopy Beyond 40 GeV

W. BUCHMÜLLER
Fermi National Accelerator Laboratory
P.O. Box 500, Batavia, Illinois 60510

ABSTRACT

The ζ -family of bound states, formed by the anticipated t-quark and its antiquark, is discussed. The quantitative connection between the ζ -spectroscopy and the short distance behavior of the quark-antiquark potential is examined. It is pointed out that the next quarkonium system will lead to an accurate determination of the QCD scale parameter Λ . Weak ζ -decays are briefly considered.

I. INTRODUCTION

Most unified models of the electroweak interactions predict the existence of a t-quark, carrying electric charge $+2/3$, which, together with the b-quark, the τ -lepton and the τ -neutrino, is supposed to build up the "third generation" of quarks and leptons. If it exists, the t-quark will be heavier^{1,2} than 19 GeV and the superheavy resonances $\zeta, \zeta', \zeta'', \dots$, formed as $(t\bar{t})$ bound states³ below the OZI threshold, can be expected to provide an ideal laboratory to test predictions of perturbative QCD and to study the weak interactions⁴ of heavy quarks.

The charmonium model⁵ was inspired by the idea of asymptotic freedom which suggests that heavy quarks and antiquarks should form non-relativistic positronium-like bound states. However, the analysis of the quarkonium spectroscopies which have been discovered so far, i.e. the Ψ and T families, has not led to unequivocal evidence⁶ for asymptotic freedom. It is expected that the next quarkonium system will settle this issue, and most of this talk will be concerned with the question what we can learn about the short distance behavior of the $(Q\bar{Q})$ potential from the ζ -spectroscopy. In addition, weak decays will be briefly discussed, mainly in connection with the leptonic widths of $(t\bar{t})$ resonances and the feasibility of observing them in e^+e^- storage rings.

II. THE $(Q\bar{Q})$ POTENTIAL AT INTERMEDIATE DISTANCES

Over the past six years the potential model for heavy quarkonia has been extensively developed. The theoretical efforts have been concentrated on the exploration of specific potential models^{7,8} as well as the application of rigorous methods derived from non-relativistic quantum mechanics.^{9,10} Theoretically, based on strong and weak coupling expansions in QCD, one expects the static $(Q\bar{Q})$ potential to be Coulombic at short distances and to become linear at large quark-antiquark separation. The "Coulomb plus linear" potential, which is obtained by a simple superposition of both asymptotic limits, therefore represents the prototype of a QCD-like potential model, and its detailed study by the Cornell group¹¹ has led to a successful description of the Ψ and Υ families.

More recently, various authors have investigated the effects of logarithmic modifications¹² of the Coulombic part of the potential which are expected as a result of vacuum polarization corrections in QCD. Richardson,¹² in particular, has obtained a simple and elegant potential which yields an excellent description of the $(c\bar{c})$ - and $(b\bar{b})$ -spectra. In order to relate the short distance behavior of the $(Q\bar{Q})$ potential to a well-defined QCD scale parameter, say $\Lambda_{\overline{MS}}$,¹³ the two-loop contribution to the β -function and the one-loop correction to the potential have to be incorporated consistently. These considerations led to a new potential model¹⁴ and, within this framework, to a value of $\Lambda_{\overline{MS}} = 0.5$ GeV which, determined from quarkonium spectroscopy, is consistent with analyses¹⁵ of deep inelastic scattering experiments.

QCD-like potential models have achieved a successful description of the Ψ and Υ spectroscopies, in particular with respect to leptonic widths¹⁴ and hyperfine splittings which are most sensitive to the short distance part of the $(Q\bar{Q})$ potential. However, this success is not unique. It is shared with the class of logarithmic and

small power potentials, investigated in detail by Quigg and Rosner¹⁶ and Martin,¹⁷ which do not conform to the theoretical expectations at either small or large distances. Thus, so far quarkonia have not led to any conclusive evidence for the theoretical preconceptions based on QCD. Yet the Ψ and T families have determined the quark-antiquark potential at intermediate distances: the four phenomenologically successful potentials, shown in Fig. 1, all coincide numerically at distances r with $0.1 \text{ fm} \leq r \leq 1.0 \text{ fm}$, although their functional forms are very different. At large and small distances a variety of asymptotic behaviors appear to be compatible with present experimental data.

The evidence for a flavor independent^{19,20} $(Q\bar{Q})$ potential has also been established in a model independent way by use of the inverse scattering method. Using mass differences and leptonic widths of the S-states in the Ψ or T families as input and assuming different "correction factors"²⁰ in the van Royen-Weisskopf formula (which reflect uncertainties of unknown relativistic and higher order radiative corrections), the $(Q\bar{Q})$ potential has been constructed. Again, as shown in Fig. 2, it appears to be uniquely determined at distances between 0.1 fm and 1.0 fm where it coincides with the specific models shown in Fig. 1. The accuracy to which potential models can account for the properties of quarkonia is demonstrated by table I, where the predictions of various models for the three narrow S-states of the T family have been compiled.

The discussion of this section leads to the following conclusions:

(i) QCD-like potential models provide an accurate description of the Ψ and T families. However, this success is shared with power potentials, which disagree with theoretical expectations based on QCD. Thus, no direct unequivocal evidence for asymptotic freedom has been obtained so far on the basis of quarkonia.

(ii) The $(Q\bar{Q})$ potential has emerged as a measurable quantity, which can be directly compared with predictions derived from any fundamental theory of strong

interactions. The Ψ and T spectroscopies have determined the quark-antiquark potential at distances between 0.1 fm and 1.0 fm.

III. THE $(Q\bar{Q})$ POTENTIAL AT SHORT DISTANCES

At short distances the $(Q\bar{Q})$ potential can be computed perturbatively in QCD. The result^{14,21} reads (for 4 flavors)

$$V^{\text{QCD}}(r) \underset{r \rightarrow 0}{\sim} -\frac{4}{3} \frac{\alpha_s(r)}{r} ,$$

$$\alpha_s(r) = \frac{12\pi}{25t} \left[1 - \frac{462}{625} \frac{\ln t}{t} + \left(\frac{53}{75} + 2\gamma_E \right) \frac{1}{t} + \mathcal{O}\left(\frac{1}{t^2}\right) \right] , \quad (3.1)$$

$$t = \ln \frac{1}{r^2 \Lambda_{\overline{\text{MS}}}^2} ,$$

where $\gamma_E = 0.5772\dots$ is Euler's constant. In order to compare this perturbative short distance behavior with a phenomenological potential, one has to specify at what distances corrections to Eq. (3.1) are expected to be negligible. In analyses of deep inelastic scattering processes comparison with perturbative QCD is considered to be justified for momentum transfers Q , which satisfy $Q^2/\Lambda^2 > 100$. Correspondingly, at distances r , with

$$r < r_c , \quad \frac{1}{r_c^2 \Lambda_{\overline{\text{MS}}}^2} = 100 \quad . \quad (3.2)$$

$V^{\text{QCD}}(r)$ should be a good approximation to the $(Q\bar{Q})$ potential. Indeed, for distances $r < r_c$, the corrections of relative order $1/t$ in Eq. (3.1) are less than $\sim 15\%$ and the perturbation series is self-consistent. Nonperturbative effects, such

as gluonic vacuum fluctuations, characterized by a nonvanishing expectation value $\phi \equiv \langle 0 | \frac{\alpha_s}{\pi} G_{\mu\nu} G^{\mu\nu} | 0 \rangle$,²² appear to be negligible; a dimensional analysis¹⁴ suggests corrections less than 1%.

Figure 3 shows $V^{\text{QCD}}(r)$ for different values of $\Lambda_{\overline{\text{MS}}}$ and distances $r < r_c$; for comparison the potentials of Martin¹⁷ and Ref. 14 are also given. For $\Lambda_{\overline{\text{MS}}} = 0.1$ GeV, $V^{\text{QCD}}(r)$ and the empirical potential, determined by the Ψ and Υ families, overlap for distances between 0.1 fm and 0.2 fm. The two potentials appear to be clearly different in this region, and a quantitative analysis¹⁴ shows that values of $\Lambda_{\overline{\text{MS}}}$ less than or equal to 0.1 GeV appear indeed incompatible with quarkonium spectroscopy. For values $\Lambda_{\overline{\text{MS}}} > 0.2$ GeV perturbation theory becomes unreliable already at distances $r < 0.1$ fm. Therefore present quarkonia cannot distinguish in a model independent way between values of $\Lambda_{\overline{\text{MS}}}$ larger than 0.2 GeV.

Obviously, the ζ -spectroscopy will be sensitive to larger values of the scale parameter. Figure 4 shows two potentials whose asymptotic behaviors at short distances are characterized by the scale parameters $\Lambda_{\overline{\text{MS}}} = 0.2$ GeV and $\Lambda_{\overline{\text{MS}}} = 0.5$ GeV. The indicated mean square radii illustrate down to which distances the $(Q\bar{Q})$ potential will be probed by $(t\bar{t})$ bound states of a given mass. The properties of the 1S-state of the ζ -spectroscopy will be most sensitive to the short distance part of the potential. Figure 5 shows the 1S-2S mass difference as a function of the t -quark mass for $\Lambda_{\overline{\text{MS}}} = 0.2$ GeV, $\Lambda_{\overline{\text{MS}}} = 0.5$ GeV and Martin's potential;¹⁷ for a t -quark mass of 30 GeV various predictions of the different models are listed in table II. It appears obvious that a $(t\bar{t})$ system with $m_\zeta \geq 40$ GeV will clearly distinguish between power potentials and QCD-like models as well as between different values of $\Lambda_{\overline{\text{MS}}}$.

The main problem in the determination of Λ by means of the $(Q\bar{Q})$ potential is the uncertainty in the absolute normalization of the potential, i.e. the uncertainty in our knowledge of the c-quark and b-quark masses. The ζ -spectroscopy will measure the $(Q\bar{Q})$ potential down to distances of about 0.04 fm, where a change of $\Lambda_{\overline{MS}}$ by 100 MeV will change the "asymptotic freedom" potential by about 300 MeV. The uncertainty in the absolute normalization of the empirical potential of about ± 400 MeV (cf. Fig. 1) will lead to an uncertainty of about ± 150 MeV in the determination of Λ . This situation would be improved through a better theoretical understanding of fine structure, hyperfine structure and E1 transitions which would lead to a more precise determination of the quark masses.

It is also conceivable that the scale parameter will be determined more accurately through the measurement of electromagnetic and hadronic decay widths, where next to leading order QCD radiative corrections have recently been computed.^{23,24} For instance, a measurement of the hadronic width of a 60 GeV toponium state with an accuracy of $\sim 20\%$ would determine the strong coupling constant of $\alpha_s(60 \text{ GeV})$ within $\sim 7\%$ and thereby measure $\Lambda_{\overline{MS}}$ with an uncertainty of about ± 100 MeV. This, in turn, would fix the normalization of the $(Q\bar{Q})$ potential up to ± 300 MeV and thereby determine the c-quark and b-quark masses within ± 150 MeV!

Thus the ζ -spectroscopy will not just determine the $(Q\bar{Q})$ potential at short distances and the QCD scale parameter Λ , it will also have consequences for the Ψ and T spectroscopies: we can expect a better determination of the c- and b-quark masses and a very accurate test of the flavor-independence of the potential at intermediate distances due to the large number of ζ -states with mean square radii in this region. For instance, as shown in Fig. 6, a $(t\bar{t})$ system of 60 GeV will have 8-9 narrow S-states, in accord with the semiclassical estimate²⁵

$$n \approx 2 \left(\frac{m_t}{m_c} \right)^{1/2}, \quad (3.3)$$

and a corresponding number of P-, D-, F-,... states which will lead to an extremely rich spectrum of electromagnetic and hadronic transitions.²⁶

Predictions for the ζ -spectroscopy up to ground-state masses of 60 GeV have also been made in a model independent way based on inverse scattering methods.²⁷ The three potentials, shown in Fig. 2, which are constructed from the masses and leptonic widths of the T family, lead to a range of predictions for toponium, thus reflecting the degree to which the ζ -spectroscopy can already be anticipated from our understanding of the T-spectroscopy. The energy level spacings of the first four S-states are shown in Fig. 7. The main conclusion is that the properties of the 1S ground state, in particular its leptonic width, will be most important for the determination of the short distance behavior of the $(Q\bar{Q})$ potential.

The main results of this section can be summarized as follows:

(i) $V^{\text{QCD}}(r)$, the "asymptotic freedom" potential calculated in perturbative QCD, is expected to coincide with the empirical $(Q\bar{Q})$ potential at distances $r < r_c$, where $1/r_c^2 \Lambda_{\overline{\text{MS}}}^2 = 100$;

(ii) the Ψ and T spectroscopies lead to the lower bound on the QCD scale parameter Λ , $\Lambda_{\overline{\text{MS}}} > 0.1 \text{ GeV}$;

(iii) the ζ -spectroscopy, with $m_\zeta > 40 \text{ GeV}$, will determine the scale parameter Λ , if $\Lambda_{\overline{\text{MS}}} < 0.5 \text{ GeV}$;

(iv) the ζ -spectroscopy may lead to a better determination of the c-quark and b-quark masses;

(v) the properties of the 1S toponium ground state will most conclusively determine the short distance behavior of the $(Q\bar{Q})$ potential.

IV. WEAK DECAYS

It has been noted by many authors²⁸⁻³¹ that weak decays of quarkonia become very important as the mass of the constituent quark increases. Of particular importance are neutral current effects on the leptonic decay widths which determine the production cross section of quarkonia in e^+e^- collisions.

The decay modes of spin-1 S-states, which occur to leading order in the strong and electroweak coupling constants, are shown in Fig. 8. They fall into two categories: annihilation decays (cf. Figs. 8a-8e), which are proportional to the wave function at the origin squared, and single quark decays (cf. Fig. 8f). The various partial decay widths of the ζ ground state are listed in table III for a t-quark mass of 30 GeV. It is very intriguing that, contrary to our experience with the Ψ and T spectroscopies, the electroweak decays dominate the strong decays! We also note that the branching ratio of the decay into Higgs particle and photon has become substantial.

Two examples may illustrate the interesting phenomena which can be expected in ζ -decays as a result of the increased strength of the weak interactions:

(a) The vector meson D^{*0} decays mostly via the strong and electromagnetic decays $D^{*0} \rightarrow D^0\pi^0$ and $D^{*0} \rightarrow D^0\gamma$. For heavier constituent quarks, such as a (t \bar{b}) system, which can form the vector and pseudoscalar states T_b^* and T_b , a different decay pattern is predicted, because the hyperfine splitting $M(T_b^*) - M(T_b)$ is expected to be smaller than the pion mass. Thus the strong decay $T_b^* \rightarrow T_b\pi^0$ is kinematically forbidden, and the M1-transition $T_b^* \rightarrow T_b\gamma$ is also suppressed, due to the small momentum of the emitted photon. As pointed out by Bigi and Krasemann,³¹ T_b^* is therefore anticipated to decay mostly via weak annihilation (cf. Fig. 9), yielding as one possible final state a very energetic lepton, which will be a rather spectacular signature.

(b) Sehgal and Zerwas³² have investigated the process (cf. Fig. 10)

$$e^+e^- \rightarrow \zeta \rightarrow b\bar{b} \quad ,$$

and the possibility to observe the interesting phenomenon of γ - Z - W interference. They find that the charged current contribution enhances the branching ratio of $b\bar{b}$ final states compared to all two-jet events,

$$\text{BR} = \frac{\sigma(e^+e^- \rightarrow \zeta \rightarrow b\bar{b})}{\sigma(e^+e^- \rightarrow \zeta \rightarrow \Sigma q\bar{q})} \quad ,$$

by more than 50% for ζ -masses around 50 GeV. Above 70 GeV the Z contribution becomes dominant.

The strong, electromagnetic and weak contributions to the ζ -decay width are shown as a function of m_ζ in Fig. 11. Clearly, three different regions have to be distinguished:

$$(1) \quad m_\zeta < m_Z$$

$$(2) \quad m_\zeta \sim m_Z$$

$$(3) \quad m_\zeta > m_Z \quad .$$

In the first case, $m_\zeta < m_Z$, the ζ -spectroscopy will look similar to the Ψ and T families. There is, however, the problem that the spread in beam energy may wash out the expected resonance structure. The integral of the ratio

$$R = \frac{\sigma(e^+e^- \rightarrow \Sigma f\bar{f})}{\sigma(e^+e^- \rightarrow \gamma^* \rightarrow \mu^+\mu^-)} \quad (4.1)$$

with respect to the cms energy over a single resonance is given by

$$\int R dE \sim \frac{9\pi}{2\alpha^2} \Gamma_{ee} \quad (4.2)$$

If δE is one standard deviation of the beam energy spread, the corresponding peak value in R reads

$$R_{\text{peak}} = \frac{\int R dE}{\sqrt{2\pi}\delta E} \quad (4.3)$$

As an illustration, for $\delta E = 100 \text{ MeV} \times (E/100 \text{ GeV})^2$ one obtains

$$R_{\text{peak}} = 1.06 \left(\frac{100 \text{ GeV}}{m_\zeta} \right)^2 \Gamma(\zeta \rightarrow \gamma^*, Z^* \rightarrow e^+e^-, \text{ in keV}) \quad (4.4)$$

Figure 12 shows R_{peak} of the ζ -ground state as a function of m_ζ , and the non-resonant background R at the corresponding energy. Due to the quadratic increase of δE with E , R_{peak} becomes smaller than the background at $m_\zeta \sim 70 \text{ GeV}$.

At $m_\zeta \sim m_Z$, R_{peak} amounts to only $\sim 10\%$ of R . However, both the signal and the background are strongly enhanced as a consequence of the Z -pole. Due to high statistics a characteristic $Z - \zeta$ interference pattern³⁴ may be observable.

In the case $m_\zeta > m_Z$ quarkonium physics will be very difficult. As Goggi and Penso³⁰ have pointed out, it may be feasible because of the dominance of the single quark decay in this mass region (cf. Fig. 11), which is expected to yield high spereocity events in contrast to the entirely two-jet like background.

V. SUMMARY

The main conclusions are as follows:

(1) The $(Q\bar{Q})$ potential has emerged as a measurable quantity, which allows a comparison with QCD at all coupling strengths. The Ψ and T spectroscopies have determined the potential at distances between 0.1 fm and 1.0 fm.

(2) Comparison of the "asymptotic freedom" potential of perturbative QCD with the empirical $(Q\bar{Q})$ potential, determined by Ψ and T data, leads to a lower bound on the QCD scale parameter, $\Lambda_{\overline{MS}} > 0.1$ GeV. The ζ -spectroscopy, with $m_\zeta > 40$ GeV, will determine the $(Q\bar{Q})$ potential down to distances of ~ 0.04 fm. If $\Lambda_{\overline{MS}} < 0.5$ GeV, as expected on the basis of deep inelastic scattering processes, this will lead to a determination of the QCD scale parameter Λ .

(3) The ζ -spectroscopy will have important consequences for Ψ and T physics. It will provide a very accurate test of the flavor-independence of the $(Q\bar{Q})$ potential at intermediate distances and may also lead to a more precise determination of the c-quark and b-quark masses.

(4) ζ -decays will be dominated by weak interactions. A variety of interesting phenomena, such as γ - Z - W interference can be anticipated.

Thus the ζ -spectroscopy will provide an ideal laboratory to study the theories of strong and electroweak interactions.

ACKNOWLEDGMENTS

The author is indebted to G. Grunberg and H. Tye for lively collaboration on most of the topics mentioned here. Helpful discussions with W. Bardeen, J.D. Bjorken, S. Gottlieb and C. Quigg, and the kind hospitality of the theory group at the Fermi National Accelerator Laboratory are gratefully acknowledged.

FOOTNOTES AND REFERENCES

- ¹ Ch. Berger, et al. (PLUTO Collaboration), Phys. Lett. 91B, 148 (1980); R. Brandelik, et al. (TASSO Collaboration), Z. Phys. C4, 87 (1980); W. Bartel, et al. (JADE Collaboration), Phys. Lett. 91B, 152 (1980); D.P. Barber, et al. (MARK-J Collaboration), Phys. Rev. Lett. 44, 1722 (1980).
- ² Recent theoretical contributions include M. Krammer, M. Voloshin and V. Zakharov, Phys. Lett. 93B, 447 (1980); S.L. Glashow, Phys. Rev. Lett. 45, 1914 (1980); B. Pendleton and G.G. Ross, Oxford University preprint (1980); C.T. Hill, Fermilab-Pub-80/97 (1980); A.J. Buras, Fermilab-Pub-81/27 (1981).
- ³ For a general discussion of toponium physics, see E. Eichten, these proceedings; J. Ellis, Proceedings of the LEP Summer Study, CERN 79-01, 662 (1979).
- ⁴ Weak decays of heavy quarkonia are discussed in detail by J. Leveille, these proceedings; J.H. Kühn, preprint MPI-PAE/PTh 37/80 (1980).
- ⁵ T. Appelquist and D.H. Politzer, Phys. Rev. Lett. 34, 43 (1975).
- ⁶ The present status of quarkonium physics and the relation to QCD has been summarized by K. Gottfried, Cornell preprint CLNS 80/467 (1980).
- ⁷ For recent reviews, see C. Quigg in Proceedings of the 1979 International Symposium on Lepton and Photon Interactions at High Energies, T. Kirk and H. Abarbanel, ed. (Fermilab, Batavia, Illinois, 1979); K. Gottfried in Proceedings of the International Symposium on High Energy e^+e^- Interactions, Vanderbilt University, Nashville, Tennessee, 1980; K. Berkelman in Proceedings of the XXth International Conference on High Energy Physics, Madison, Wisconsin, 1980.
- ⁸ General reviews of the theory are given in T. Appelquist, R.M. Barnett, and K.D. Lane, Ann. Rev. Nucl. Sci. 28, 387 (1978); M. Krammer and H. Krasemann in

- New Phenomena in Lepton-Hadron-Physics, D. Fries and J. Wess, ed. (Plenum, New York and London, 1979); J.D. Bjorken in Proceedings of the 1979 SLAC Summer Institute on Particle Physics, SLAC report no. 224 (Ed. A. Mosher); J.L. Rosner, Lectures at Advanced Studies Institute on Techniques and Concepts of High Energy Physics, St. Croix, Virgin Islands, 1980.
- ⁹ C. Quigg and J.L. Rosner, Phys.Rep. 56, 167 (1979).
- ¹⁰ H. Grosse and A. Martin, Phys. Rep. 60, 341 (1980); R.A. Bertlmann and A. Martin, Nucl. Phys. B168, 111 (1980).
- ¹¹ E. Eichten, K. Gottfried, T. Kinoshita, K.D. Lane and T.M. Yan, Phys. Rev. D17, 3090 (1978); D21, 203 (1980).
- ¹² A representative list includes W. Celmaster, H. Georgi and M. Machacek, Phys. Rev. D17, 879 (1978); W. Celmaster and F.S. Henyey, Phys. Rev. D18, 1688 (1978); A. Billoire and A. Morel, Nucl. Phys. B135, 131 (1978); B. Margolis, R. Roskies and N. De Takacsy, Paper submitted to IV European Antiproton Conference, Barr, France (1978); J.L. Richardson, Phys. Lett. 82B, 272 (1979); H. Krasemann and S. Ono, Nucl. Phys. B154, 283 (1979); M. Kramer, H. Krasemann and S. Ono, preprint DESY 80/25 (1980); R.D. Carlitz, D.B. Creamer and R. Roskies, unpublished; R.D. Carlitz and D.B. Creamer, Ann. Phys. (N.Y.) 118, 429 (1979); R. Levine and Y. Tomozawa, Phys. Rev. D19, 1572 (1979) and D21, 840 (1980); J. Rafelski and R.D. Viollier, Ref. TH.2673-CERN (1979) and MIT preprints CTP 791, 819 (1979); G. Fogleman, D.B. Lichtenberg and J.G. Wills, Nuovo Cimento Lett. 26, 369 (1979).
- ¹³ The $\overline{\text{MS}}$ -scheme was introduced in W.A. Bardeen, A. Buras, D.W. Duke and T. Muta, Phys. Rev. D18, 3998 (1978). For a review see A. Buras, Rev. Mod. Phys. 52, 199 (1980). The relations between $\Lambda_{\overline{\text{MS}}}$, $\Lambda_{\overline{\text{MS}}}$ and Λ_{MOM} read

$\Lambda_{\overline{MS}} = 0.377 \Lambda_{\overline{MS}}$, $\Lambda_{MOM} = 2.16 \Lambda_{\overline{MS}}$, see W. Celmaster and R.J. Gonsalves, Phys. Rev. Lett. 42, 1435 (1979) and Phys. Rev. D20, 1420 (1979).

¹⁴W. Buchmüller, G. Grunberg and S.-H.H. Tye, Phys. Rev. Lett. 45, 103 (1980); 45, 587 (E) (1980); W. Buchmüller and S.-H.H. Tye, preprint Fermilab-Pub-80/94-THY (1980).

¹⁵For a recent review, see A.J. Buras, preprint Fermilab-Conf-80/79-THY, to be published in Physica Scripta.

¹⁶C. Quigg and J.L. Rosner, Phys. Lett. 71B, 153 (1977); M. Machacek and Y. Tomozawa, Prog. Theor. Phys. 58, 1890 (1977) and Ann. Phys. (N.Y.) 110, 407 (1978).

¹⁷A. Martin, Phys. Lett. 93B, 338 (1980); Ref. TH.2980-CERN (1980); for earlier work on power potentials, see M. Machacek and Y. Tomozawa, Ann. Phys. 110, 407 (1978); C. Quigg and J.L. Rosner, Comments Nucl. Part. Phys. 8, 11 (1978).

¹⁸G. Bhanot and S. Rudaz, Phys. Lett. 78B, 119 (1978).

¹⁹C. Quigg, H.B. Thacker and J.L. Rosner, Phys. Rev. D21, 234 (1980); C. Quigg and J.L. Rosner, Fermilab-Conf-80/75-THY (to appear in Proc. XXth International Conference on High Energy Physics, Madison, 1980).

²⁰C. Quigg and J.L. Rosner, Fermilab-Pub-81/13-THY (1981).

²¹W. Fischler, Nucl. Phys. B129, 157 (1977); A. Billoire, Phys. Lett. 92B, 343 (1980).

²²M.A. Shifman, A.I. Vainshtein and V.I. Zakharov, Nucl. Phys. B147, 385, 448 (1979). With respect to the size of ϕ , see, however, W. Wetzel, Heidelberg report HD-THEP-79-15 (1980).

²³R. Barbieri, G. Curci, E. d'Emilio and E. Remiddi, Nucl. Phys. B154, 535 (1979); R. Barbieri, M. Caffo, R. Gatto and E. Remiddi, Phys. Lett. 95B, 93 (1980); P. Mackenzie and G.P. Lepage, in preparation.

- ²⁴For a recent review, see E. Remiddi, Lectures given at the International School of Physics E. Fermi, Varenna 1980, preprint IFUB-2/81 (1981).
- ²⁵C. Quigg and J.L. Rosner, Phys. Lett. 72B, 462 (1978).
- ²⁶For new results on hadronic transitions in the ζ -spectroscopy, see T.M. Yan, these proceedings.
- ²⁷P. Moxhay, J.L. Rosner and C. Quigg, preprint Fermilab-Pub-81/14-THY (1981).
- ²⁸J. Ellis and M.K. Gaillard, report CERN 76-18 (1976).
- ²⁹K. Fujikawa, Prog. Theor. Phys. 61, 1186 (1979).
- ³⁰G. Goggi and G. Penso, Nucl. Phys. B165, 429 (1980).
- ³¹I.I.Y. Bigi and H. Krasemann, Z. Phys. C7, 127 (1981).
- ³²L.M. Sehgal and P.M. Zerwas, Aachen preprint PITHA 80-11 (1980). For related work of Fischbach, Kayser and Wolfram, see E. Fischbach, Proc. "Neutrinos-78," ed. E.C. Fowler (Purdue University, 1978), p. 467.
- ³³J.H. Kühn, ref. 4.
- ³⁴F.M. Renard, Z. Phys. C1, 225 (1979).

Table I. Predictions of various potential models for the T family, compared with experiment. Model 1: Martin¹⁷; model 2: Buchmüller, Grunberg and Tye,¹⁴ $\Lambda_{\overline{MS}} = 0.5$ GeV; model 3: Richardson¹²; model 4: Bhanot and Rudaz¹⁸ (the range of predictions, which are dependent on the b-quark mass, is given); model 5: Cornell group.¹¹

The first column contains the leptonic widths in keV, the second and third columns the excitation energies in MeV and, in brackets, the ratios of the leptonic widths with respect to the T leptonic width.

From Ref. 14.

	T	T'	T''
Experiment			
a) Ref. 5	1.29 ± 0.22	553 ± 10 (0.45 ± 0.08)	---
b) Ref. 6, 7	1.02 ± 0.22 1.10 ± 0.17	560 ± 3 (0.45 ± 0.07)	889 ± 4 (0.32 ± 0.06)
Model 1 (Martin)	---	560 (0.43)	890 (0.28)
Model 2 (Buchmüller, Grunberg & Tye)	1.07	555 (0.46)	890 (0.32)
Model 3 (Richardson)	---	555 (0.42)	886 (0.30)
Model 4 (Bhanot and Rudaz)	1.07 - 1.77	561 - 566 (0.47 - 0.76)	881 - 879 (0.34 - 0.51)
Model 5 (Cornell group)	---	560 (0.48)	898 (0.34)

Table II. Comparison of $(t\bar{t})$ spectra for different potential models, with $m_t = 30$ GeV.

	Martin ¹⁷	$\Lambda_{\overline{MS}}=0.2 \text{ GeV}^{14}$	$\Lambda_{\overline{MS}}=0.5 \text{ GeV}^{14}$	Richardson ¹²
$E_2 - E_1$ [MeV]	512	610	762	801
$\Gamma_{ee}(2S)/\Gamma_{ee}(1S)$	0.48	0.43	0.30	0.29
$E_3 - E_1$ [MeV]	814	913	1090	1136
$\Gamma_{ee}(3S)/\Gamma_{ee}(1S)$	0.34	0.28	0.18	0.17

Table III. Strong and electroweak partial decay widths of the ζ -ground state with $m_t = 30$ GeV; the various processes are displayed in Fig. 8. The values $\alpha_s(60 \text{ GeV}) = 0.137$ and $\Gamma_{ee}(\zeta) = 5 \text{ keV}$ have been assumed.

final state	e^+e^-	3g	$\gamma, 2g$	$H\gamma$	$\Sigma f\bar{f}(\gamma^*, Z^*)$	$b(\bar{b})W$
Γ (keV)	5	24.4	3.8	1.6	31.0	10.1

FIGURE CAPTIONS

- Fig. 1: Various successful potentials are shown. The numbers refer to the following references: (1) Martin, Ref. 17; (2) Buchmüller, Grunberg and Tye, Ref. 14; (3) Bhanot and Rudaz, Ref. 18; (4) Cornell group, Ref. 11. The potentials (1), (3) and (4) have been shifted to coincide with (2) at $r = 0.5$ fm; the "error bars" indicate the uncertainty in absolute, r -independent normalization. States of the Ψ and T families are displayed at their mean square radii. From ref. 14.
- Fig. 2: Three potentials constructed from T data by means of the inverse scattering method, corresponding to three different "correction factors" ρ in the van Royen-Weisskopf formula, $\Gamma_{ee}(nS) = 1/\rho (16 \pi \alpha^2 e_Q^2)/M_n^2 |\phi_n(0)|^2$. Dot-dashed line: $\rho = 1.0$; solid line: $\rho = 1.4$; long-dashed line: $\rho = 2$. The short-dashed line is the QCD-like potential of ref. 14, with the scale parameter chosen as $\Lambda_{\overline{MS}} = 0.5$ GeV. From ref. 20.
- Fig. 3: 2-loop "asymptotic freedom" potentials for 4 flavors and different values of $\Lambda_{\overline{MS}}$ at distances $r \leq r_c$, $r_c^2 = 1/(100 \Lambda_{\overline{MS}}^2)$. For comparison the potentials (1) and (2) of Fig. 1 are also displayed. The "error bars" indicate the uncertainty with respect to absolute normalization. From ref. 14.
- Fig. 4: Two ($Q\bar{Q}$) potentials which approach "asymptotic freedom" potentials with $\Lambda_{\overline{MS}} = 200$ MeV and $\Lambda_{\overline{MS}} = 500$ MeV at short distances. Mean square radii of ($t\bar{t}$) ground states (denoted as $\zeta(2m_t)$) are shown for $\Lambda_{\overline{MS}} = 500$ MeV and different quark masses m_t . From ref. 14.

- Fig. 5: 1S-2S mass differences as function of t-quark mass m_t . The solid lines represent the potentials of Fig. 4, the dashed line Martin's potential.¹⁷ From ref. 14.
- Fig. 6: Energy level spacings of $(t\bar{t})$ bound states in several potentials. (a) Inverse scattering, $\rho = 1$; (b) inverse scattering, $\rho = 1.4$; (c) inverse scattering, $\rho = 2$; (d) Richardson potential, ref. 12; (e) QCD-like model of ref. 14, with $\Lambda_{\overline{MS}} = 0.2$ GeV; (f) QCD-like model of ref. 14, with $\Lambda_{\overline{MS}} = 0.5$ GeV. From ref. 27.
- Fig. 7: $(t\bar{t})$ S-wave bound states below threshold as function of the t-quark mass. The binding energies have been computed for a potential which corresponds to $\Lambda_{\overline{MS}} = 300$ MeV; it satisfies $V(\Lambda_{\overline{MS}} = 200 \text{ MeV}) \geq V(\Lambda_{\overline{MS}} = 300 \text{ MeV}) \geq V(\Lambda_{\overline{MS}} = 500 \text{ MeV})$. From ref. 14.
- Fig. 8: Decays of $(t\bar{t})$ resonances with $J^{PC} = 1^{--}$ to leading order in the strong and electroweak coupling constants. g = gluon, γ = photon, f = fermion, q = quark, H = Higgs particle.
- Fig. 9: Weak annihilation of $T_b^* = (t\bar{b})$ into quark--or lepton--pairs.
- Fig. 10: γ - Z - W interference in the process $e^+e^- \rightarrow \zeta \rightarrow b\bar{b}$.
- Fig. 11: Electromagnetic, electroweak and strong decay widths as functions of m_ζ . The sum over all fermions f in the final state has been performed, and a constant decay width $\Gamma(\zeta \rightarrow \gamma^* \rightarrow \mu^+\mu^-)$ of 5 keV has been assumed. (This value lies in between the predictions of the QCD-like models of ref. 14, with scale parameters $\Lambda_{\overline{MS}} = 0.2$ GeV and $\Lambda_{\overline{MS}} = 0.5$ GeV.) In the single quark decay, $\zeta \rightarrow b(\bar{b})W$, propagator effects have been neglected. For a detailed discussion, see J.H. Kühn, ref. 4.

Fig. 12:

R_{peak} , the contribution to R of the ζ -ground state as a function of m_ζ (cf. Eqs. (4.1), (4.3)) compared to the non-resonant value of R . The sum over all fermions f in the final state has been performed, and a constant decay width $\Gamma(\zeta \rightarrow \gamma^* \rightarrow \mu^+ \mu^-)$ of 5 keV has been assumed.

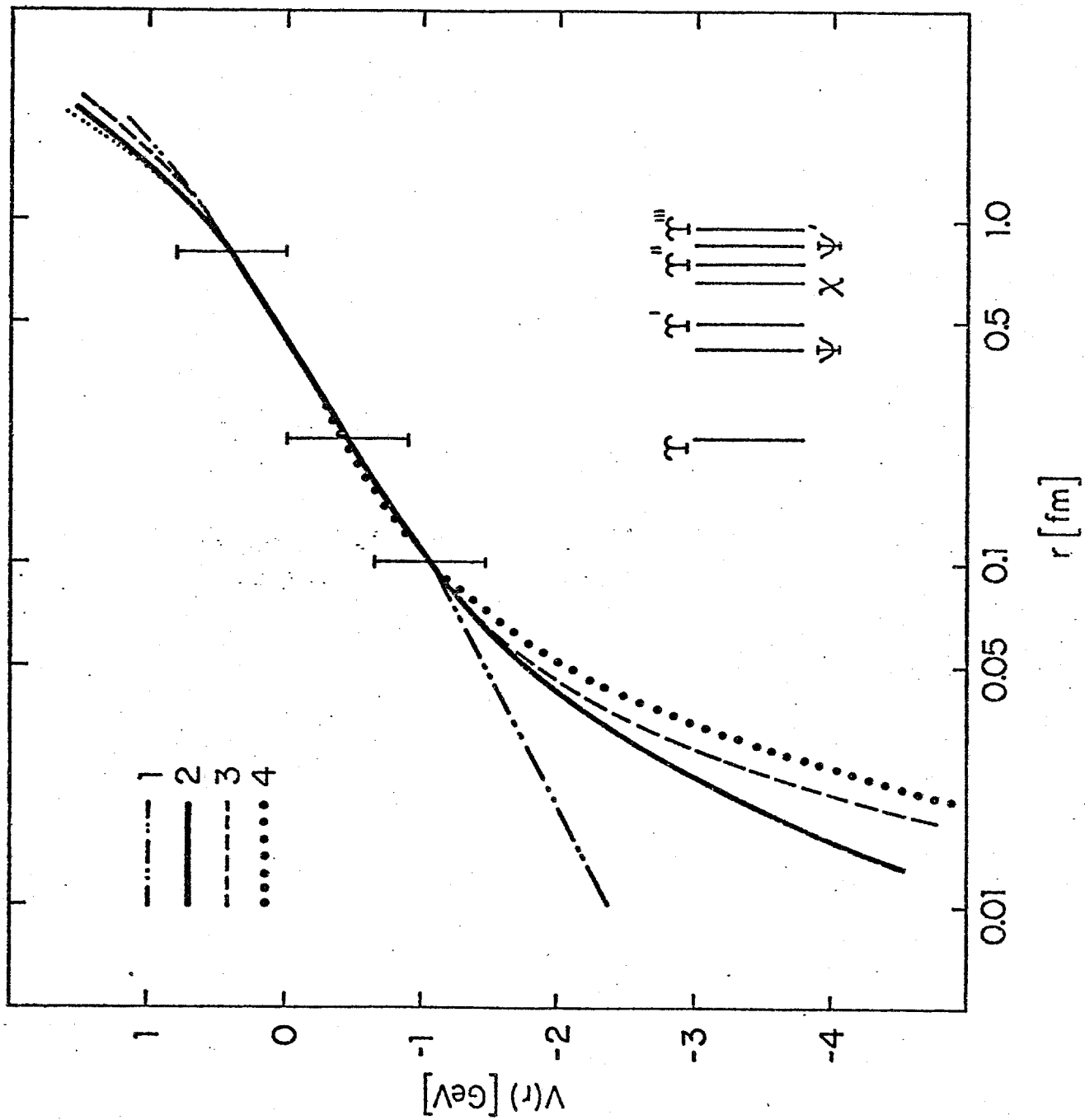


Fig. 1

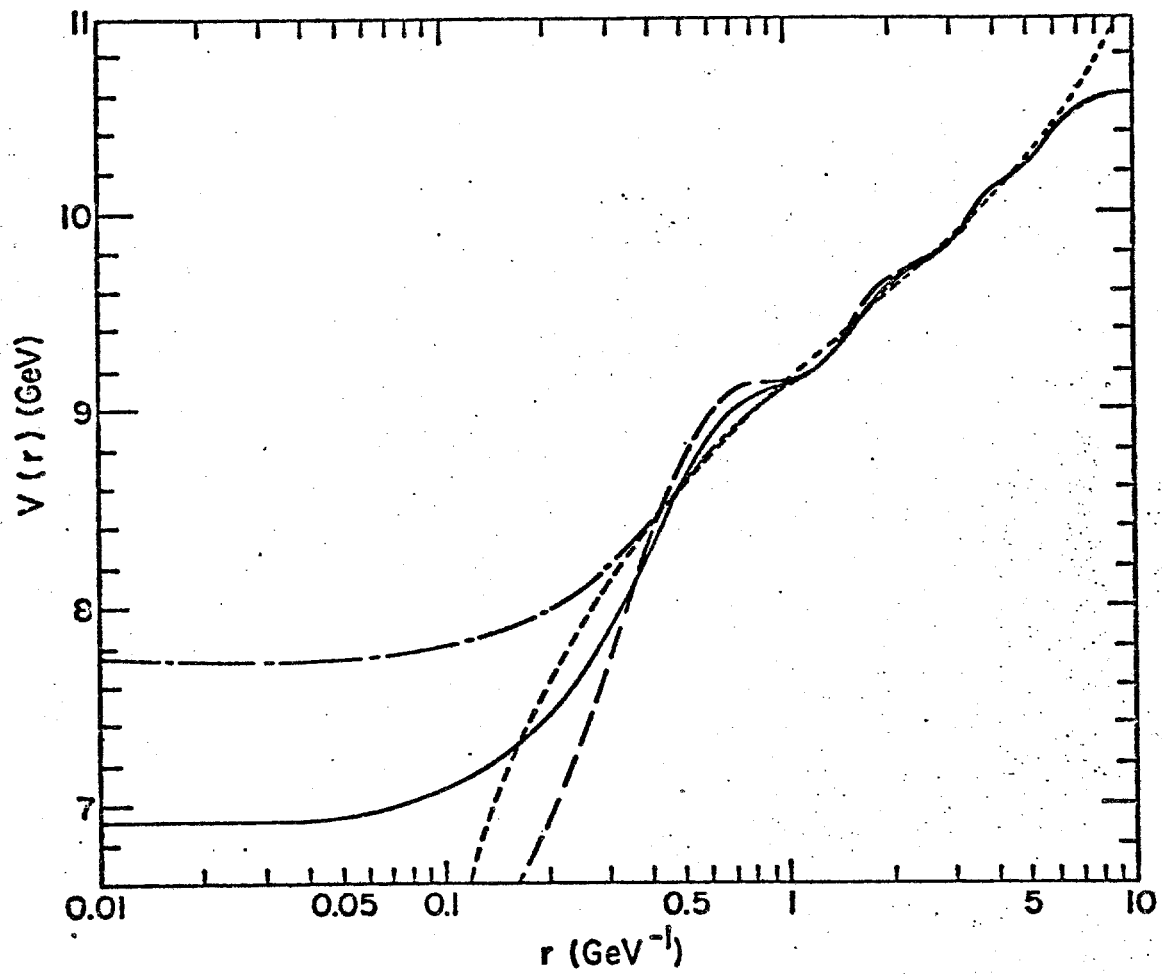


Fig. 2

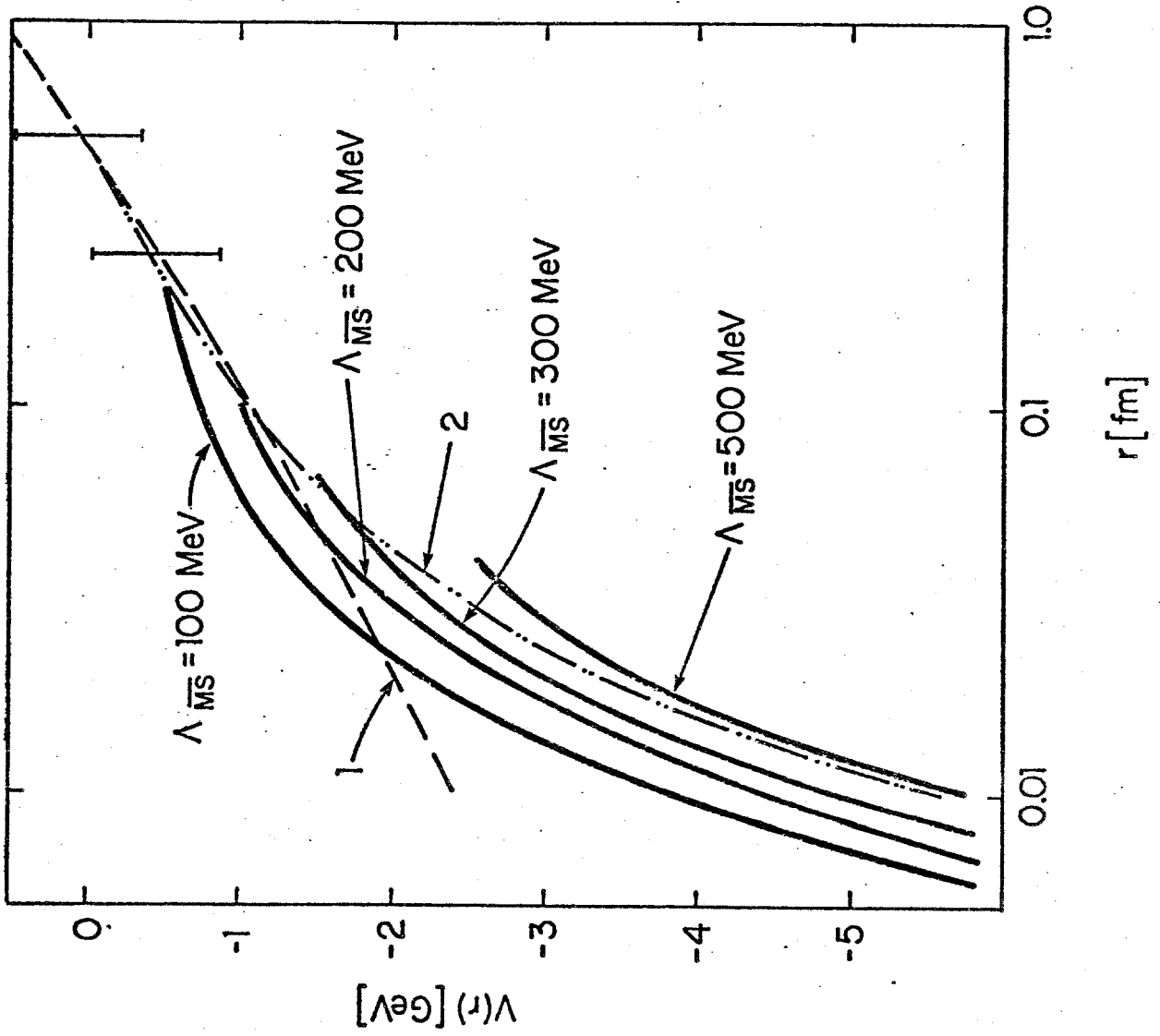


Fig. 3

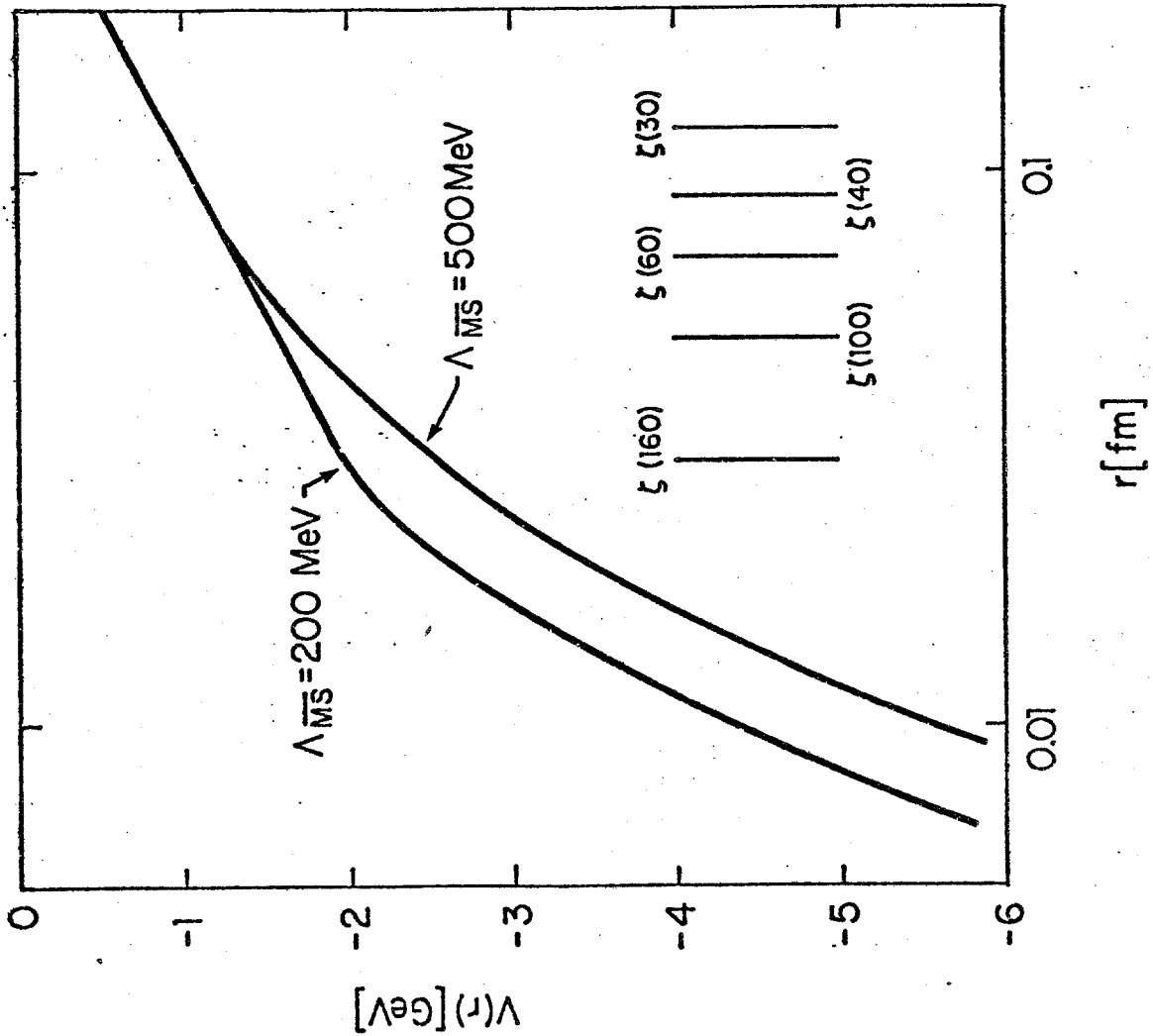


Fig. 4

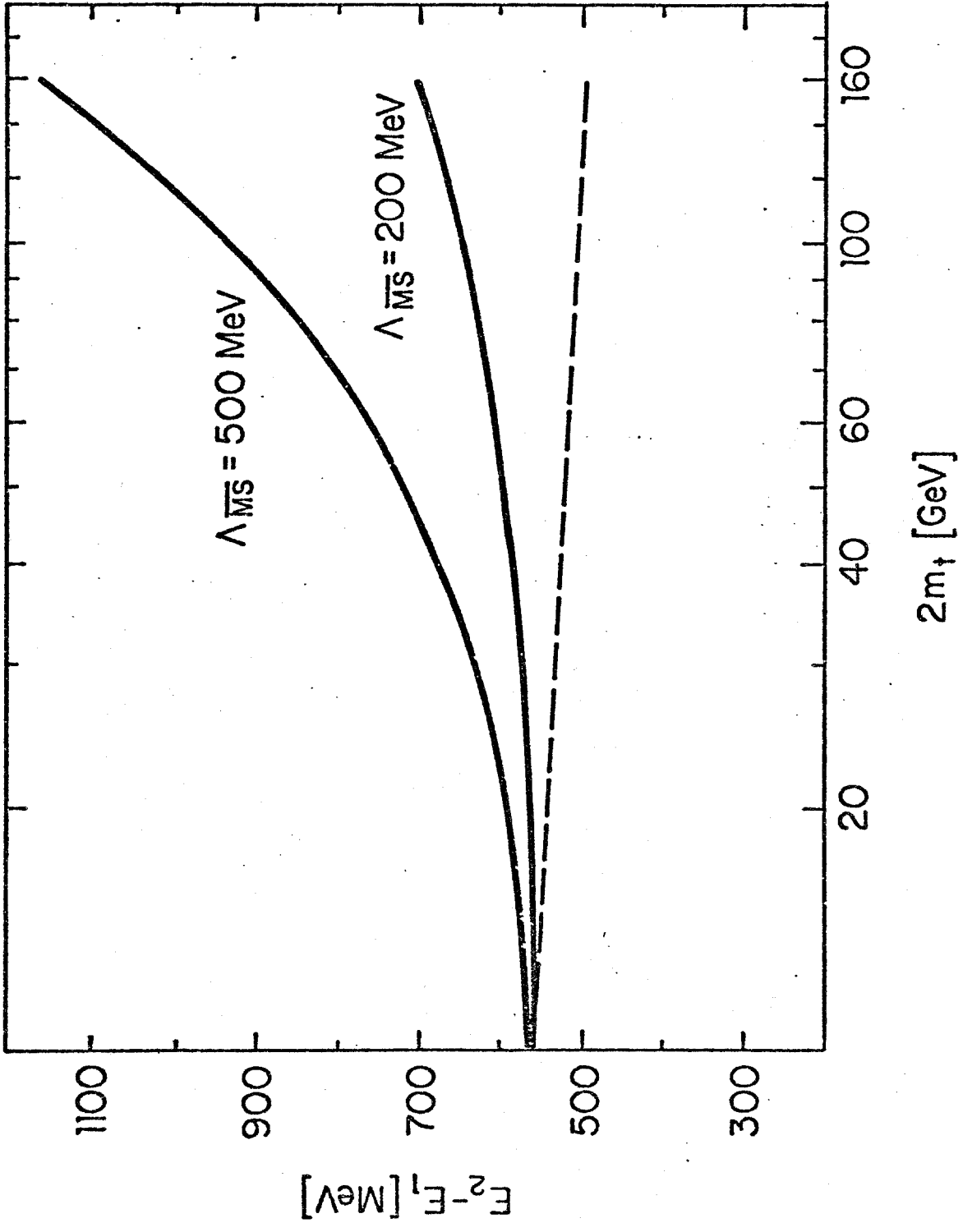


Fig. 5

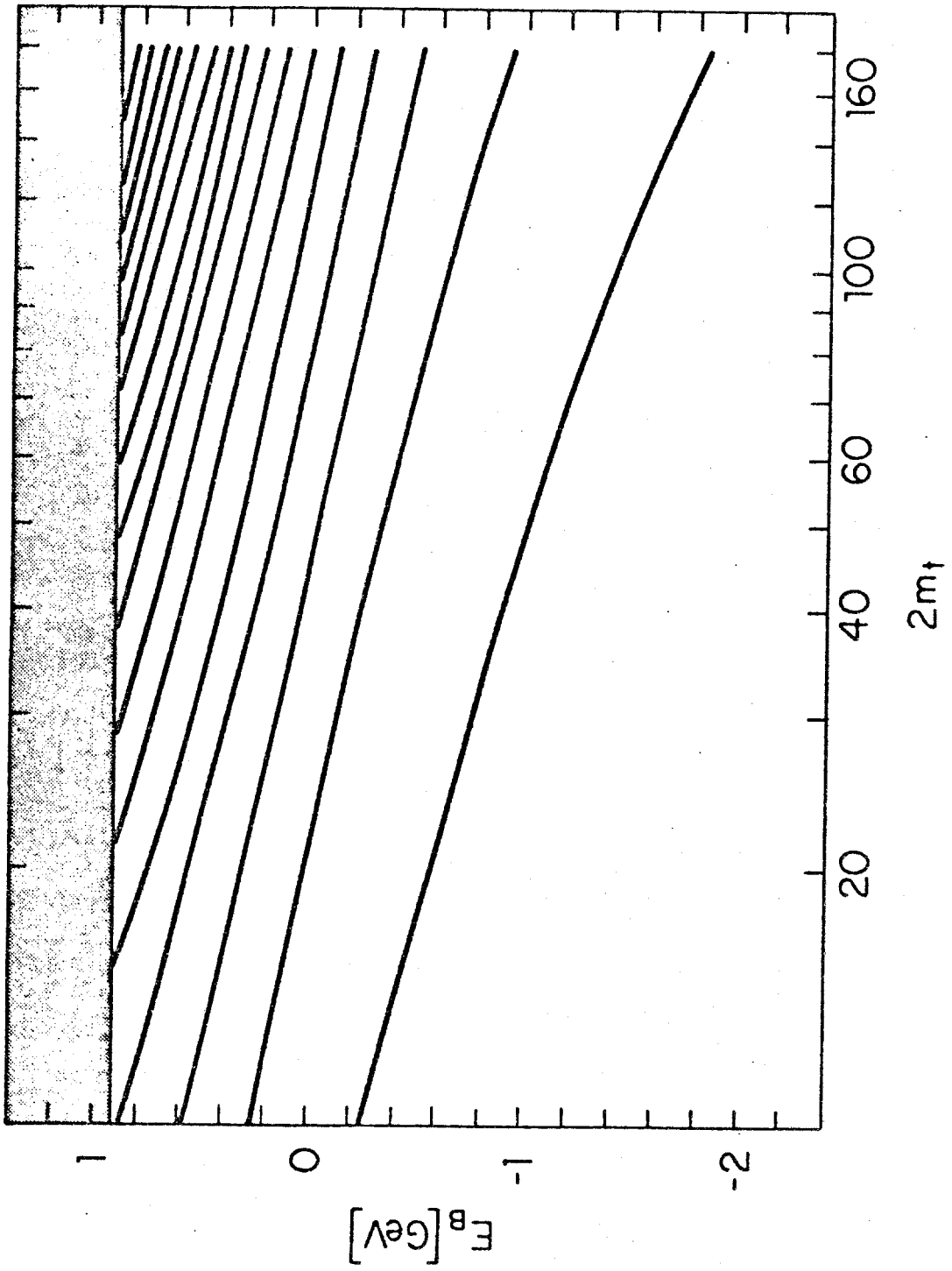


Fig. 6

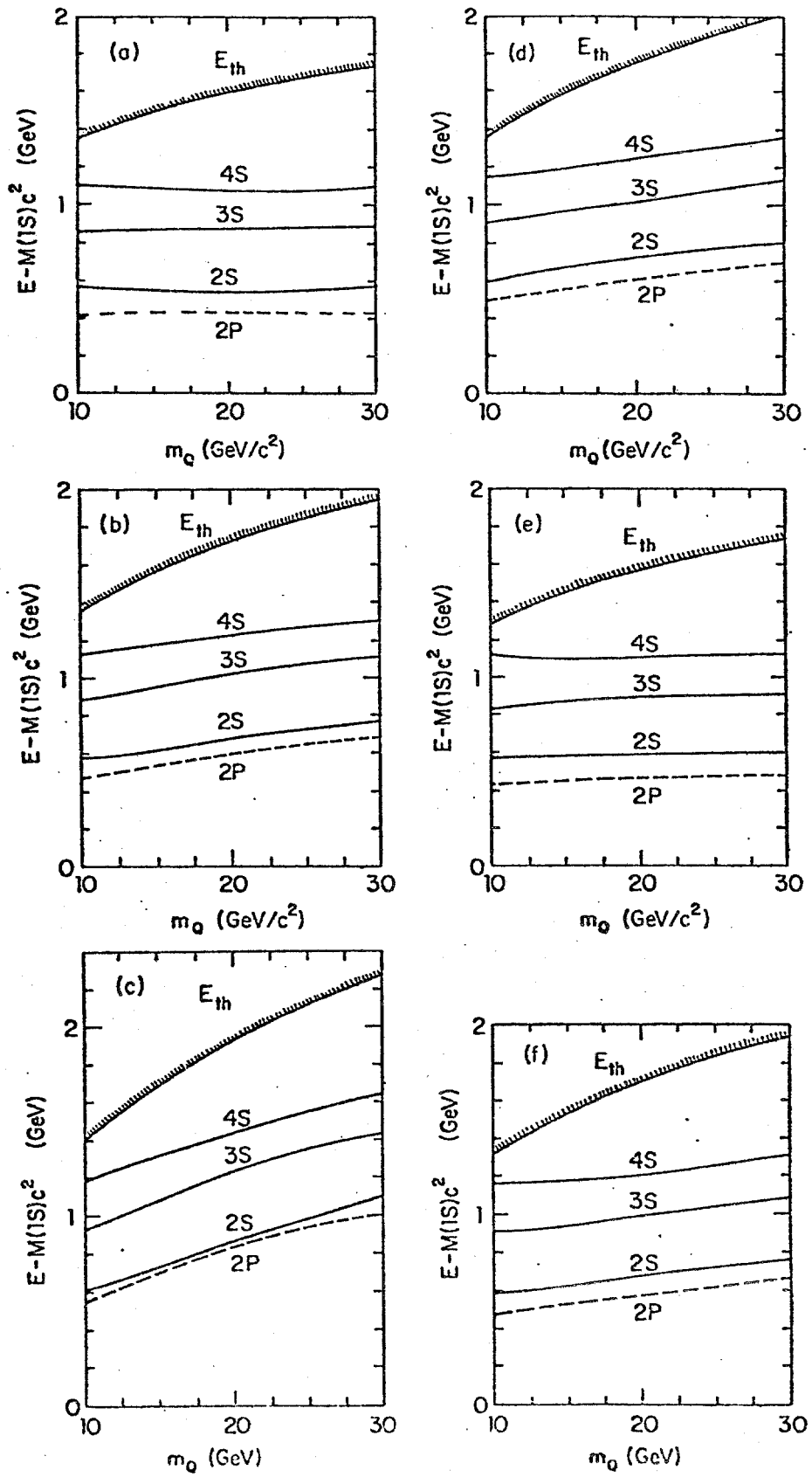
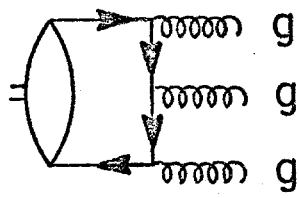
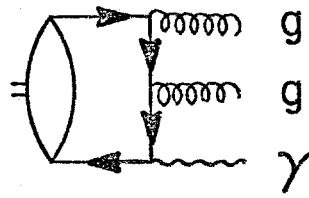


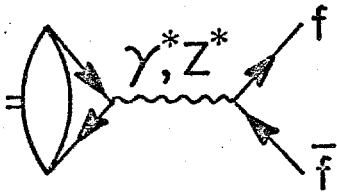
Fig. 7



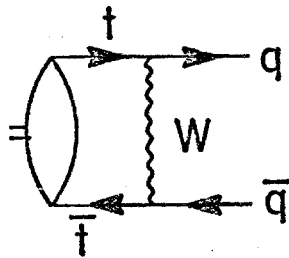
(a)



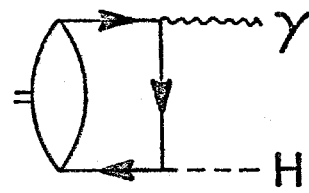
(b)



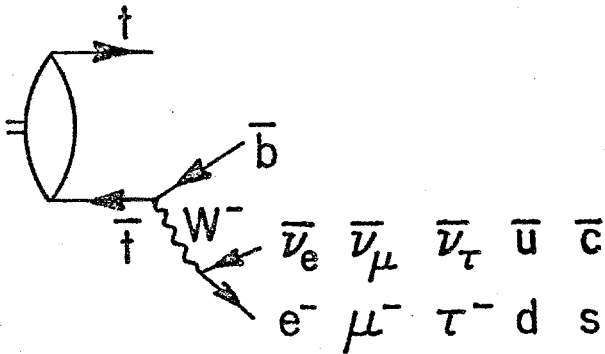
(c)



(d)



(e)



(f)

Fig. 8

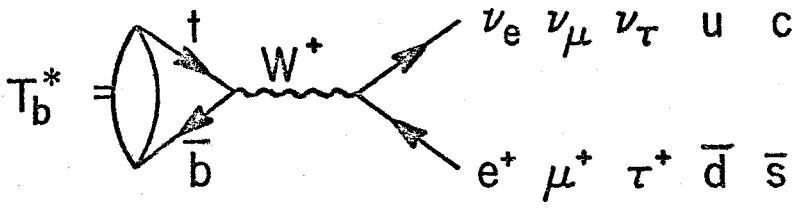


Fig. 9

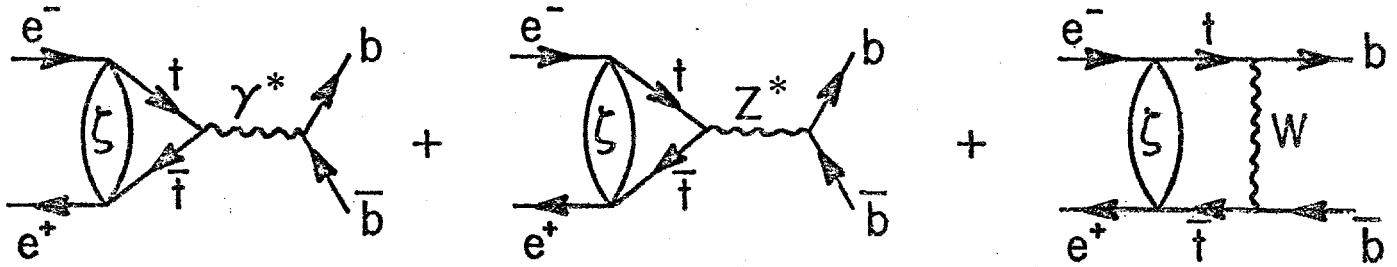


Fig. 10

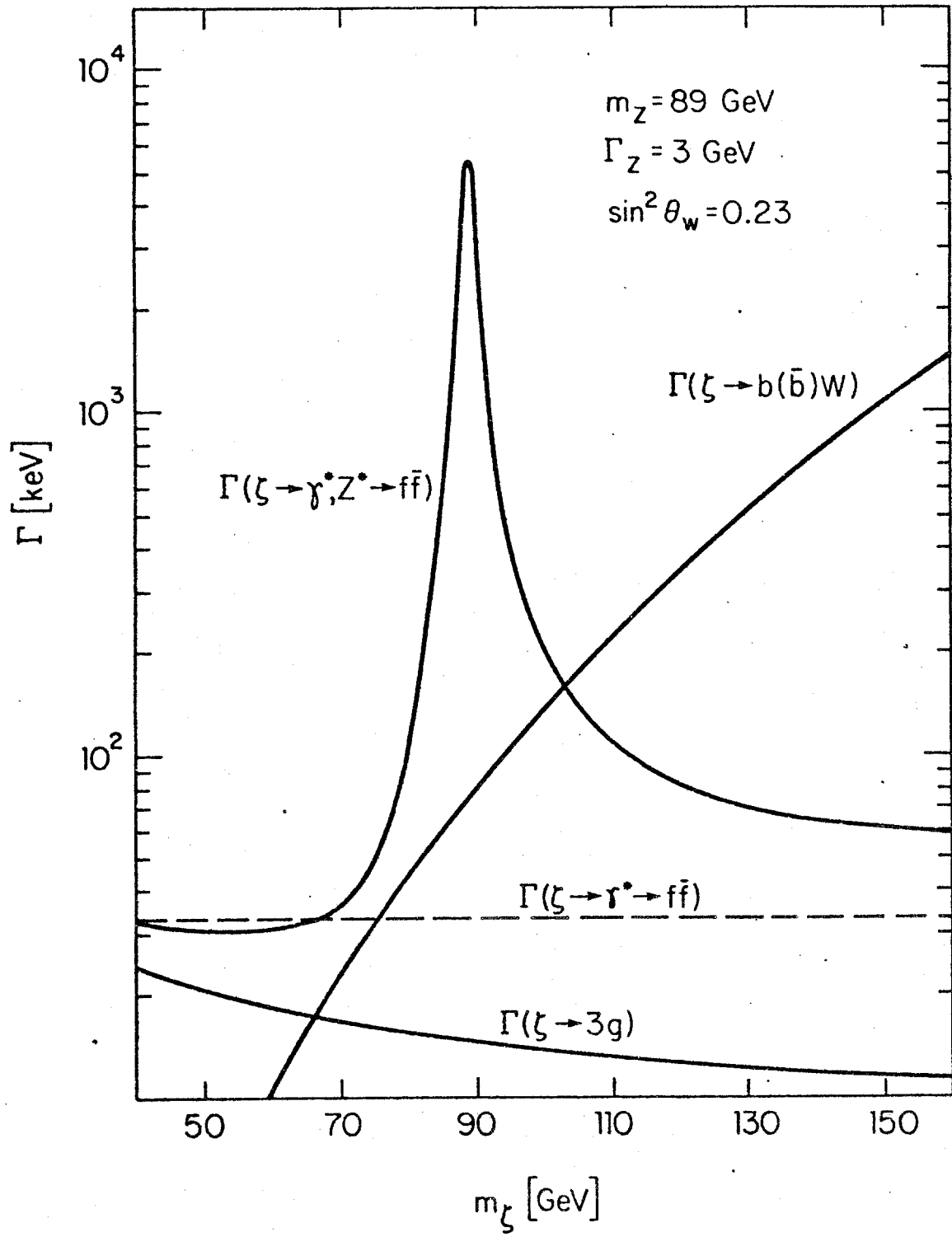


Fig. 11

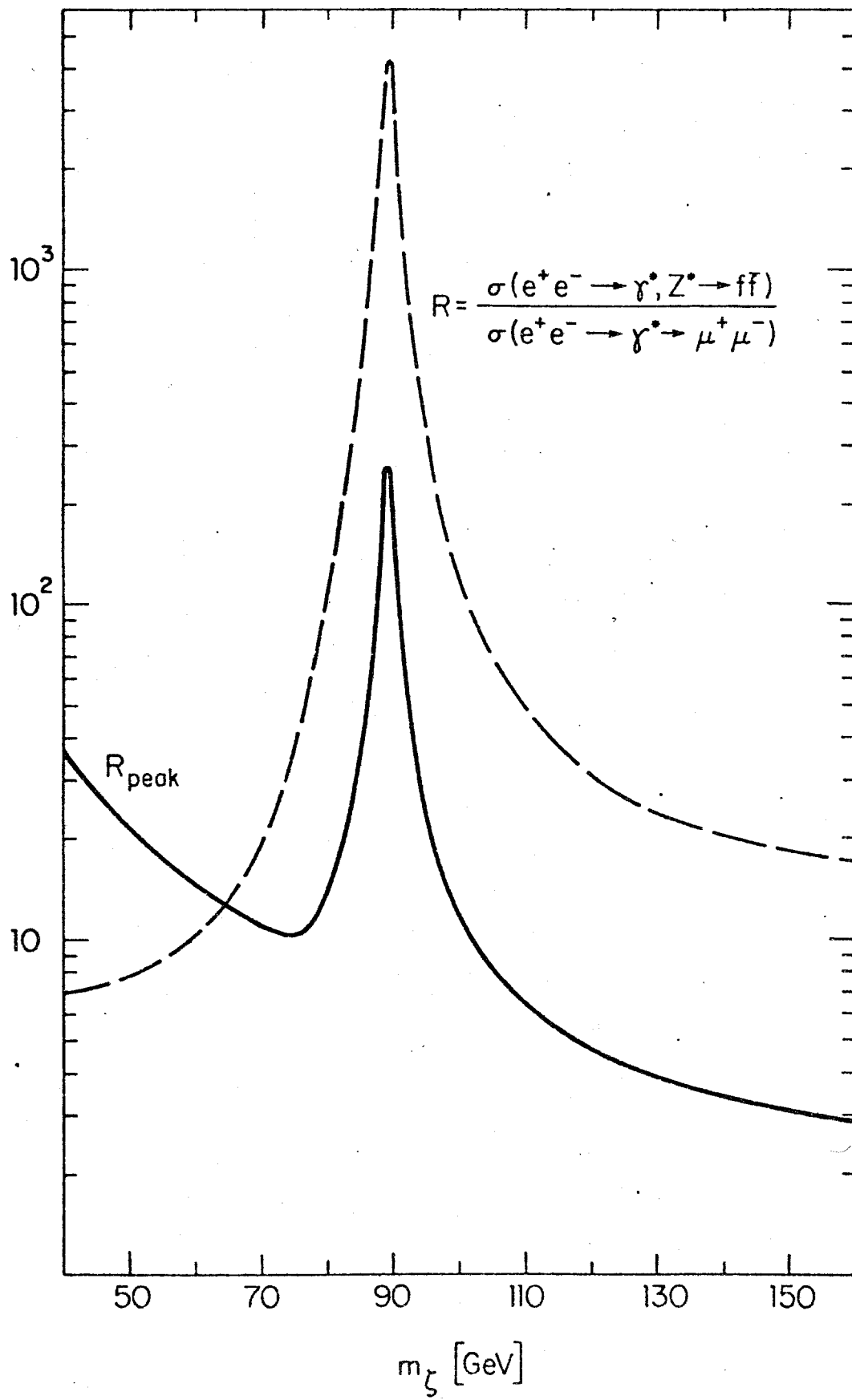


Fig. 12